


Direct radiative effects of aerosols over South Asia from observations and modeling

Vijayakumar S. Nair¹  · S. Suresh Babu¹ · M. R. Manoj¹ · K. Krishna Moorthy² · Mian Chin³

Received: 1 April 2016 / Accepted: 2 October 2016
© Springer-Verlag Berlin Heidelberg 2016

Abstract Quantitative assessment of the seasonal variations in the direct radiative effect (DRE) of composite aerosols as well as the constituent species over the Indian sub continent has been carried out using a synergy of observations from a dense network of ground based aerosol observatories and modeling based on chemical transport model simulations. Seasonal variation of aerosol constituents depict significant influence of anthropogenic aerosol sources in winter and the dominance of natural sources in spring, even though the aerosol optical depth doesn't change significantly between these two seasons. A significant increase in the surface cooling and atmospheric warming has been observed as season changes from winter ($DRE_{SUR} = -28 \pm 12 \text{ W m}^{-2}$ and $DRE_{ATM} = +19.6 \pm 9 \text{ W m}^{-2}$) to spring ($DRE_{SUR} = -33.7 \pm 12 \text{ W m}^{-2}$ and $DRE_{ATM} = +27 \pm 9 \text{ W m}^{-2}$). Interestingly, springtime aerosols are more absorptive in nature compared to winter and consequently the aerosol induced diabatic heating of the atmosphere goes as high as $\sim 1 \text{ K day}^{-1}$ during spring, especially over eastern India. The atmospheric DRE due to dust aerosols ($+14 \pm 7 \text{ W m}^{-2}$) during spring overwhelms that of black carbon DRE ($+11.8 \pm 6 \text{ W m}^{-2}$) during winter. The DRE at the top of the atmosphere is mostly governed by the anthropogenic aerosols during all the seasons. The columnar aerosol loading, its anthropogenic fraction and radiative effects shows a steady increase with latitude across Indian

mainland leading to a larger aerosol-induced atmospheric warming during spring than in winter.

Keywords Aerosol radiative effect · Black carbon · Dust · Anthropogenic aerosols

1 Introduction

Atmospheric aerosols perturb the radiation balance of the earth atmosphere system directly through interaction with radiation (Haywood and Boucher 2000) and indirectly by aerosol-cloud (Lohmann and Feichter 2005) and aerosol-cryosphere interactions (Flanner et al. 2007). The large demographic pressure and increasing demand for the energy and fresh water call for the better understanding of the plausible pathways of aerosol-climate interactions and its implication on the agriculture and hydrological cycle over the south Asian regions, especially over the Indian region. Even though, there are uncertainties in the magnitude and mechanisms of aerosol induced climate forcing over South Asia, the significance of aerosols on regional climate and monsoon are unequivocal. Investigations of climate impacts of aerosols over the South Asia has been extensively made using state-of-the-art models and large scale field experiments during the last two decades and several hypotheses have been put forward especially on aerosol-hydro-climate implications (Ramanathan et al. 2005; Lau et al. 2006; Moorthy et al. 2009; Lawrence and Lelieveld 2010; Bollasina et al. 2011; Vinoj et al. 2014). However, lack of observational evidences and large biases (underestimation) in the modeled aerosol fields have raised questions on the accuracy of these climate model projections (Nigam and Bollasina 2010; Nair et al. 2012). Studies on the amplification of ENSO signal due to absorbing

✉ Vijayakumar S. Nair
vijayakumarsnair@gmail.com

¹ Space Physics Laboratory, Vikram Sarabhai Space Centre, Thiruvananthapuram, India

² ISRO Headquarters, Bangalore, India

³ NASA Goddard Space Flight Center, Greenbelt, MD, USA

aerosols (Kim et al. 2015), effect of anthropogenic aerosols on tropical cyclones (Wang et al. 2014) and atmospheric heating due to dust aerosols on monsoon pattern (Vinoj et al. 2014; Lau 2014) indicate the heterogeneity of forcing pathways through which aerosols affect the regional hydrological cycle. Even though aerosols partially offset the warming due to CO₂ on a global scale, its radiative implications and climate feedbacks are significantly higher and at times may add to greenhouse warming at regional scales (e.g., Ramanathan et al. 2005; Nair et al. 2010). To focus more on the implications of aerosols on the regional hydroclimate, warming due to aerosols in the atmosphere need to be considered in detail (Hansen et al. 2005; Lau et al. 2006). Generally, IPCC (2007) reports focus more on the global implications of atmospheric aerosols and discuss its radiative perturbations at the top of the atmosphere. Several studies have shown that atmospheric warming due to natural as well as anthropogenic aerosols over the Indian region has significant implication for the large scale (monsoon) circulations, cloud properties and snow albedo of the Himalayan glaciers (Ackerman et al. 2000; Bollasina et al. 2011; Nair et al. 2013a; Vinoj et al. 2014).

Even though the wintertime haze and springtime dust storms over the Central and northern parts of the Indian subcontinent has immense significance to the day-to-day life of the millions of people in this region, assessment of radiative implications has generally been limited to station-specific composite aerosol system (for example Babu et al. 2002; Ganguly and Jayaraman 2006; Babu et al. 2007; Dey and Tripathi 2008) except Deepshikha et al. (2007). Regional scale assessment of seasonal transformation in aerosol radiative effects is non-existent over this region to the best of our knowledge. Jethva et al. (2009) have shown the large uncertainties in satellite retrievals of aerosols properties over the heterogeneous landmass owing to surface reflectance variations, while Nair et al. (2012) have reported that aerosol properties simulated using regional climate models are significant underestimates and biases are regionally heterogeneous. Performance evaluation studies have shown that regional, global and chemical transport models failed to capture the magnitude of aerosol loading over this region (Nair et al. 2012; Moorthy et al. 2013). Since the satellite retrievals and climate model simulations of aerosols properties are known to have large biases/uncertainties over the Indian region (Jethva et al. 2009; Nair et al. 2012), regional scale assessments of aerosol radiative forcings are rather limited to oceanic regions surrounding the Indian peninsula (Ramanathan et al. 2001; Moorthy et al. 2009; Nair et al. 2010). Hence it is essential to form a synergistic approach, by considering the pros and cons in each technique and dataset, to estimate the region specific and seasonal variations in radiative perturbations due to composite and its constituent species over the Indian landmass.

Heritage of regional characterization of columnar aerosol optical depth (AOD) over the Indian region has begun with Mani et al. (1969) using a network of sun-photometers. However, this activity went to dormancy until it was given a fresh thrust with the climate perspective, as a part of the ISRO-Geosphere Biosphere program under which, a network of indigenously developed multi-wavelength solar radiometer (MWR) was established in a phased manner which has evolved into the Aerosol Radiative Forcing over India NETwork (ARFINET) (Moorthy et al. 1997; Babu et al. 2013). The data collected from these stations have been used to validate remote sensing satellite retrievals and regional climate model simulations (Nair et al. 2012). One of the main objectives of the ARFI project is to estimate the direct radiative forcing (DRF) due to aerosols over the region accurately by synthesizing the data collected from the ARFINET observatories supplemented with satellite data and model simulations. However, the major challenge in the estimation of measurement-based DRF from ARFINET data is the lack of measurements of columnar aerosol single scattering albedo (SSA) and asymmetry parameter/phase function. The former parameter decides the sign of the radiative forcing (warming or cooling) and latter significantly influences the amount of radiation scattered back to the space. These observational constraints are not only limited to the Indian region but are global in nature as well. Several techniques have been widely used to estimate the aerosol SSA and phase function, which include inversion of sky radiation measurements using multispectral radiometers (Dubovik et al. 2000), in situ measurements of vertical distribution of scattering/absorption/extinction coefficients using aircraft (Babu et al. 2016), satellite measurements (Satheesh et al. 2009), semi empirical (Moorthy et al. 2009) and using chemical transport model simulations (Chin et al. 2009).

One of the major challenges and important, but uncertain, component in mitigation studies is the assessment of radiative forcing due to each aerosol constituent. It is hard to accurately assess the radiative implications of individual aerosol constituents fully based on in situ or satellite measurements, because of the inherent technical difficulties in the 3 dimensional characterization of aerosol constituents in addition to the constraints imposed by the lack of understanding on the mixing state of aerosols and uncertainties associated with the conversion of chemical properties to optical properties of aerosols. It should be noted that most of the chemical characterizations of aerosols are limited to near the surface, and temporal evolution of the three dimensional distributions of chemical properties of aerosols are solely limited to climate model simulations, even though, there are very few attempts to validate the modeled aerosol fields using measured aerosol composition. Accurate measurements of AODs of constituent species are

virtually non-existent, though there have been some efforts in this direction (e.g., Kaufman et al. 2005; Nair et al. 2010). However, coupled chemistry models come handy for estimating aerosol constituents (Schulz et al. 2006) and to derive constituent AODs.

In this paper, we compile all the measurements from the ARFINET and other networks in the Indian region to synthesize a realistic representation of aerosol properties. Subsequently, using chemical transport model simulations, speciated aerosol DREs are estimated and synthesized to understand the spatial and seasonal changes in the composition and its radiative implications. In the following, we first describe the database used, followed by the methodology and validation of the model simulations. Characteristics of DREs would be discussed later, with special emphasis on aerosol absorption.

2 Database and simulations

2.1 Observational data

The observational data comprised of spectral AODs (in the visible and near IR) estimated from a dense network of aerosol observatories spread across the Indian landmass. It includes 27 aerosol observatories under the ARFINET providing the regular data on columnar spectral AODs at 10 wavelength bands (Babu et al. 2013); 4 stations under the Aerosol Robotic Network (AERONET) of NASA (Holben et al. 1998) and 4 stations (equipped with Preede sun-sky radiometers) under the India Meteorological Department (IMD) (Soni et al. 2014). Details of these stations are given in Table 1. Based on the geographical characteristics and prevailing meteorological conditions, all these stations are broadly grouped as (1) Peninsular India, (2) Central India, (3) Western India, (4) Eastern India, (5) Indo Gangetic Plain (IGP) and (6) Himalayan region. Two island stations, Minicoy in the Arabian Sea and Port Blair in the Bay of Bengal, are considered as the representatives of the marine environments. It should be noted that, aerosol properties over Himalayas would vary significantly with station altitude, and as such, we have further classified the stations on Himalayas as (1) Himalayan foothill stations (Nainital, Kullu, Dehradun, Ranichauri) and (2) high altitude stations (Hanle and NCO-P). The distribution of these stations and the regional groups are shown in Fig. 1.

Most of the ARFINET stations are equipped with multi-wavelength solar radiometer (MWR), developed at Space Physics Laboratory in late 1980s (Moorthy et al. 1997). This instrument measures the direct solar radiation at 10 different wavelength bands (380–1025 nm) using filter wheel arrangement and uses the Langley plot technique to estimate the optical depth of the atmosphere.

The contributions of Rayleigh scattering and absorption by water vapor and ozone are subtracted from the total optical depth to calculate the aerosol optical depth. The instrument has a field of view of 2.0° and interference filters having 5 nm FWHM (Full Width at Half Maximum) bandwidths are used to select the wavelength bands. More technical details of this instrument, uncertainties and cloud screening protocols and inter-comparison of the spectral AODs with other instruments are already available in the literature (Moorthy et al. 1997; Beegum et al. 2008; Kompalli et al. 2010; Babu et al. 2013) and hence not repeated here. Some of the ARFINET stations used hand-held Microtops sunphotometer (Solar Light Co.) for instantaneous measurements of spectral AODs during clear sky periods (Porter et al. 2001). Observations of spectral AODs were made manually by pointing the instrument to the sun at regular intervals. Similar to MWR, AERONET sunphotometer measures the AOD at different wavelengths continuously using the direct sun measurements (Holben et al. 1998) and in addition, it estimates the SSA and aerosol phase function using the periodic sky measurements (Dubovik et al. 2000). All the IMD stations are equipped with Skyradiometer (model: POM 02, Prede Co. Ltd, Japan) for making continuous measurements of direct and diffuse radiation for measuring/retrieving AOD, SSA and phase function. Measurement technique, protocol and uncertainties of Microtops, AERONET sun radiometer and Skyradiometer are available in the literature (Holben et al. 1998; Dubovik et al. 2000; Kompalli et al. 2010). The length of the dataset varies from station to station. Some of the stations have more than a decade long observations whereas a few stations are nascent with less than 3 year of observation. We have considered only those stations, where minimum 1 year round observation is available. The climatological seasonal mean values of spectral AOD from all the stations are used to estimate the DRE.

2.2 Chemical transport model

Monthly mean values of AODs, at mid visible wavelength, for black carbon (BC), organic carbon (OC), sulfate, dust (fine + coarse) and sea salt (fine + coarse) have been taken from Goddard Chemistry Aerosol Radiation and Transport Model (GOCART) simulations for the period of January 2000 to December 2007 (Chin et al. 2002, 2009, 2014). GOCART uses the meteorological data from the Modern-Era Reanalysis for Research and Applications (MERRA) produced in the Goddard Earth Observing System Data Assimilation System (GEOS DAS). The model output used in this study has 72 vertical levels and a horizontal resolution of 2.5° longitude by 2° latitude (Chin et al. 2014). The model includes emission of anthropogenic aerosols from various sources such as industrial, transport, residential,

Table 1 Details of measurement locations

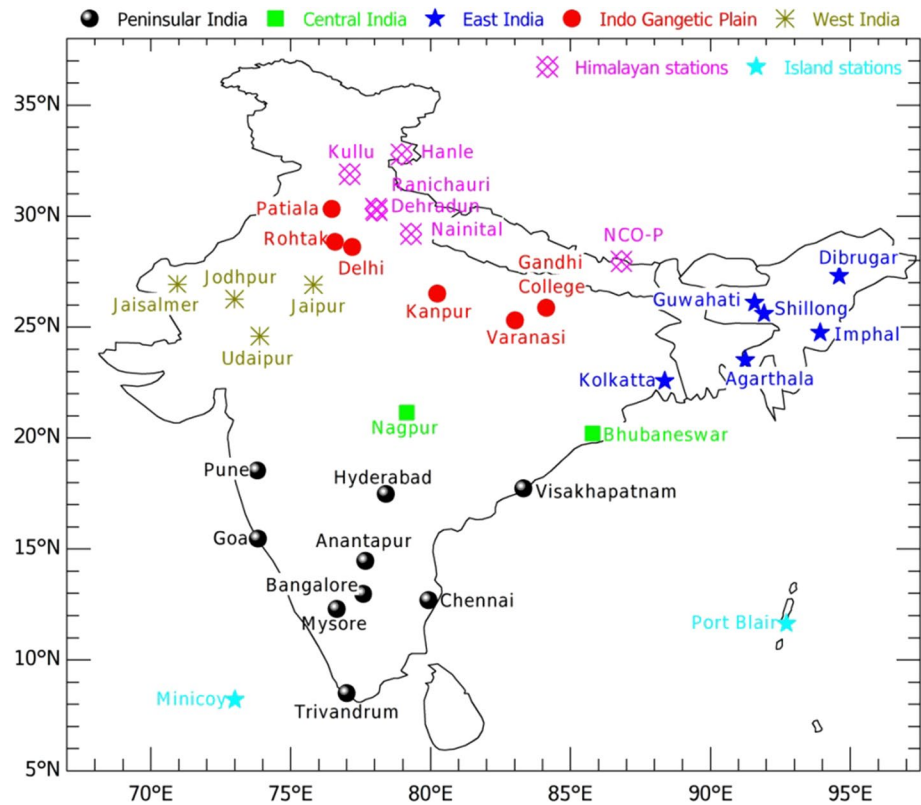
No	Station details		Region	LAT	LON	ALT	Network
	Station name	Characteristics					
1	Minicoy	Island	Oceanic	8.20	73.00	2	ARFINET
2	Port Blair	Island		11.64	92.71	60	ARFINET
3	Trivandrum	Semiurban	Peninsular India	8.50	77.00	2	ARFINET
4	Chennai	Urban		12.70	79.92	80	ARFINET
5	Bangalore	Urban		12.97	77.59	960	ARFINET
6	Anantapur	Semi arid		14.46	77.67	25	ARFINET
7	Goa	Semiurban		15.46	73.83	70	ARFINET
8	Hyderabad	Urban		17.48	78.40	557	ARFINET
9	Visakhapatnam	Semiurban		17.72	83.32	30	ARFINET
10	Mysore ^a	Semiurban		12.30	76.65	763	ARFINET
11	Pune ^a	Urban		18.5	73.8	560	ARFINET
12	Bhubaneswar	Semiurban	Central India	20.20	85.80	78	ARFINET
13	Nagpur	Urban		21.15	79.15	300	ARFINET
14	Udaipur	Semiurban	Western India	24.60	73.90	577	ARFINET
15	Jodhpur ^a	Semiurban		26.26	72.99	426	ARFINET
16	Jaisalmer	Rural		26.92	70.95	225	ARFINET
17	Jaipur	Urban		27.00	75.80	431	AERONET
18	Kolkatta	Urban	Eastern India	22.57	88.37	12	ARFINET
19	Agarthala	Rural		23.5	91.25	43	ARFINET
20	Imphal	Rural		24.75	93.92	765	ARFINET
21	Shillong	Rural		25.60	91.91	1033	ARFINET
22	Dibrugarh	Rural		27.30	94.60	111	ARFINET
23	Guwahati	Semiurban		26.1	91.58	54	IMD
24	Delhi	Urban	Indo gangetic plain	28.60	77.20	239	ARFINET
25	Patiala	Semiurban		30.33	76.46	249	ARFINET
26	Kanpur	Urban		26.5	80.2	126	AERONET
27	Gandhi College	Semiurban		25.9	84.1	60	AERONET
28	Varanasi	Semiurban		25.3	83.016	90	IMD
29	Rohtak	Rural		28.83	76.58	214	IMD
30	Nainital	Rural	Himalayan	29.20	79.30	1960	ARFINET
31	Dehradun	Semiurban		30.34	78.04	700	ARFINET
32	Kullu	Rural		31.90	77.10	1154	ARFINET
33	Hanle	Remote		32.78	78.95	4350	ARFINET
34	NCOP	Remote		28	86.80	5550	AERONET
35	Ranichauri	Rural		30.25	78.08	1800	IMD

^a Currently not working

biomass burning and natural aerosol emissions from desert, ocean and biogenic sources. Anthropogenic emission is from the ACCMIP emission inventory, which has year-to-year variation but not seasonal variation. Biomass burning emission is from the daily emission dataset of GFEDv3. Biogenic secondary organic aerosols (SOA) is estimated with the climatological monthly monoterpene emissions and assumed a 10 % yield at the point of emission. There is no anthropogenic SOA included in the version of GOCART used in this study. BC sources include anthropogenic and biomass burning and OC sources include anthropogenic,

biomass burning, and biogenic SOA (as described in Chin et al. 2002, 2009, 2014). The GOCART model treats aerosols as externally mixed due to the large uncertainties associated with the degree of internal mixing. The model assumes that BC is emitted as hydrophobic and changes to hydrophilic with an e-folding time of 1.2 days (Chin et al. 2002). The mean life time of BC is estimated as ~6 days. Recently, several studies have shown that aerosol properties changes significantly with time (aging) over urban polluted region (Peng et al. 2016; Wang et al. 2013; Zhang et al. 2015), however, these aspects are yet to be considered in

Fig. 1 Ground based observatories of sun/sky radiometers/photometers over the Indian region. Stations are classified as peninsular, central India, eastern India, Indo gangetic plain, western India, Himalayas and island stations



the chemical transport modeling. The columnar AOD and aerosol absorption optical depth (AAOD) are available at multiple wavelengths from 350 to 1500 nm. Detailed descriptions of the model, dynamics, emission sources and validation are available in Chin et al. (2014) and references therein.

3 Methodology and validation

The estimation of DRE of aerosols requires spectral variation of three major aerosol properties; (1) AOD, (2) SSA and (3) aerosol phase function or asymmetry parameter in addition to the information on vertical profiles of atmospheric parameters (temperature, water vapor and ozone) and spectral surface albedo (Moorthy et al. 2009). In this paper, we use the direct observation of AOD from the network of radiometers while SSA and phase functions are estimated from the GOCART simulations following the methodology described by Yu et al. (2004) and Chin et al. (2009).

The spectral measurements of AODs carried out using ground based radiometers/sunphotometers (MWR, hand held sunphotometer, AERONET and Skyradiometer) use different wavelengths typically ranging from 340 nm to 2000 nm. All the AOD measurements were interpolated or extrapolated to a common set of wavelengths using power

law Angstrom relationship between the AOD (τ_{obs}) and wavelength (λ).

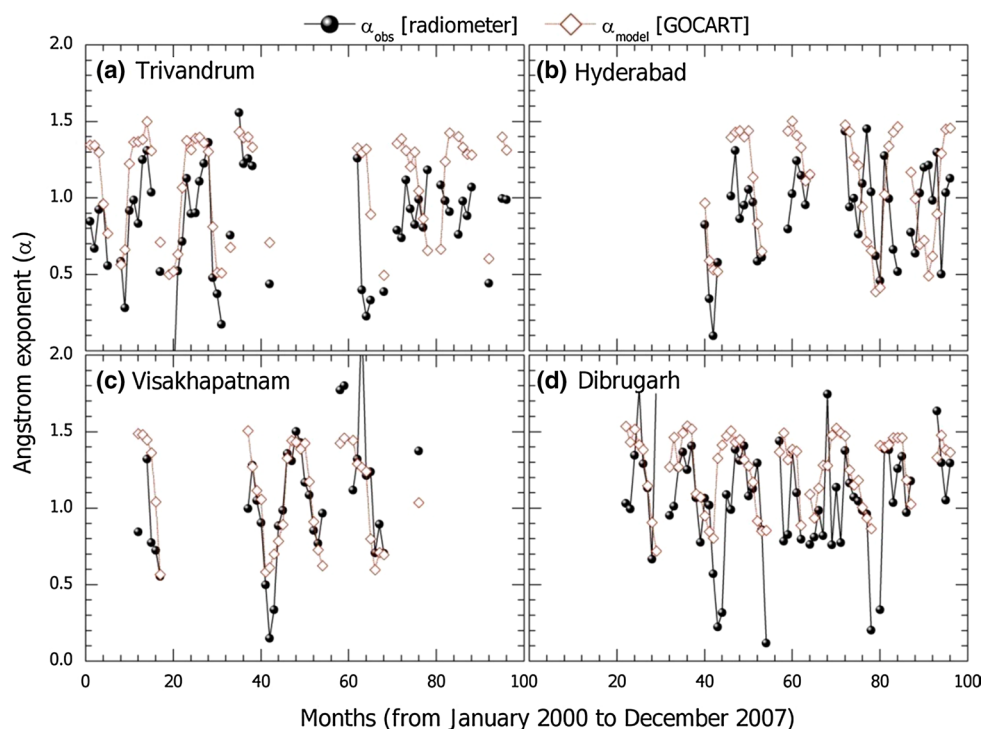
$$\tau_{obs}(\lambda) = \beta_{obs} \lambda^{-\alpha_{obs}} \quad (1)$$

where β and α are Angstrom coefficients. The Angstrom exponent (α) is widely used to qualitatively infer the dominant size region of the columnar aerosol number size distribution. Generally $\alpha > 1$ indicate fine mode dominance and $\alpha < 1$ represent coarse mode dominance in the aerosol distribution. Using Eq. 1 all the AOD measurements made using various instruments at different wavelengths were transformed to a common set of 10 wavelengths. Similarly, angstrom exponent (α_{model}) is estimated from the GOCART model simulations (using Eq. 1), where τ_{model} is the sum of individual aerosol constituent AODs (τ_i).

In contrast to AOD, columnar SSA and asymmetry parameters are poorly characterized over the Indian region and seasonal variation of these parameters do not exist over this region. The speciated aerosol fields simulated using GOCART model is used to estimate the SSA and phase function following the methodology described in Yu et al. (2004). The spectral variation of composite SSA is estimated from AOD and aerosol absorption optical depth (β_{model}) from GOCART model

$$\omega_{model}(\lambda) = 1 - \frac{\beta_{model}(\lambda)}{\tau_{model}(\lambda)} \quad (2)$$

Fig. 2 Inter comparison of Angstrom exponent estimated from the spectral measurements of aerosol optical depth using radiometers (α_{obs}) and estimated using GOCART model (α_{model}) simulations



The asymmetry parameter is estimated using the constituents AOD (τ_i) from the GOCART model and optical properties of individual aerosol species, such as SSA (ω_i) and asymmetry parameter (g_i), from Hess et al. (1998).

$$g_{\text{model}}(\lambda) = \frac{\sum_{i=1} g_i(\lambda) \omega_i(\lambda) \tau_i(\lambda)}{\sum_{i=1} \omega_i(\lambda) \tau_i(\lambda)} \quad (3)$$

Using Eqs. 1, 2 and 3, AOD, SSA and asymmetry parameter are estimated for the entire data collected from 35 stations. Considering the importance of SSA and phase function in the assessment of DRE and uncertainties associated with the Chemical Transport Model (CTM) simulations of aerosol fields over India, extensive validation of this methodology has been carried out. First, we have inter-compared the Angstrom exponents (α_{obs} and α_{model}) for the measured and modeled AODs. From the above discussion, α_{model} highly depends on the accuracy of the GOCART model simulations. Figure 2 shows the monthly mean variation of α_{obs} and α_{model} for four geographically distinct ARFINET stations (Trivandrum, Hyderabad, Visakhapatnam, Dibrugarh) during January 2000 to December 2007 period. From the figure it is clear that α_{model} matches well with α_{obs} spatially and seasonally, indicating that the GOCART model simulates the aerosol composition accurately over the sub-continent.

From the confidence gained from the above analysis, we have carried out similar analysis to validate SSA and asymmetry parameter estimated from the GOCART simulations with AERONET and IMD measurements. Figure 3

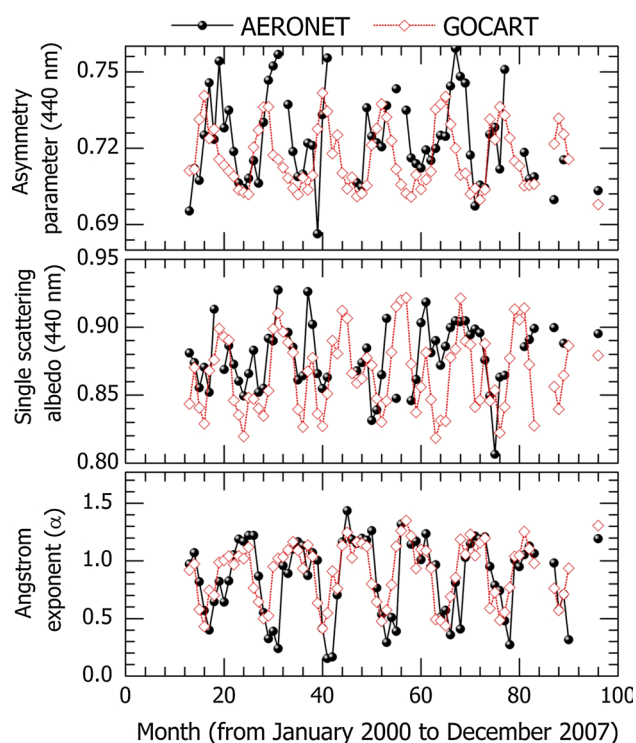


Fig. 3 Inter comparison of angstrom exponent, single scattering albedo and asymmetry parameter estimated using the GOCART simulations and retrieved from AERONET sun/sky radiometer measurements at Kanpur

shows the inter-comparison of α (bottom panel), SSA (middle panel) and asymmetry parameter (top panel) derived using AERONET sun-photometer data from Kanpur and estimated from GOCART simulations. From the figure, it emerges that this methodology has captured the seasonal variation of α , SSA and asymmetry parameter and estimated the magnitude of these parameters reasonably well. It should be noted that the SSA and asymmetry parameter measurements are not available from all the 35 stations. Unfortunately most of the stations, where SSA measurements are available (4 AERONET and 4 IMD), do not have simultaneous data during the GOCART simulation period (2000–2007). So we have shown inter-comparison results at Kanpur as a typical example to show that GOCART and AERONET observations are matching over the region. Further, we have also carried out validation of the simulated SSAs using climatological mean GOCART data (for the period 2000–2007) with observations for more stations (Gandhi College, Pune, Jaipur, Ranichauri, Rohtak, Guwahati, Varanasi). This analysis indicates a reasonable agreement in the magnitude and seasonal variation of SSA in all the stations except Pune. Similar and extensive studies have been already published by Chin et al. (2009), where these authors have inter-compared the GOCART data with various AERONET sites located at distinct aerosol environments across the globe. From Figs. 2 and 3, it is very clear that, this methodology is able to capture the aerosol size characteristics and chemical properties accurately. These validation results are highly encouraging and the aerosol model used in this paper followed this methodology for all the stations seasonally. Chin et al. (2009) have reported that even though GOCART fail to capture the absolute magnitude of aerosol loading over the IGP, it reproduced the SSA fairly well indicating the accuracy of model chemistry (fractional contribution of each species to the total AOD). AODs of the individual aerosol species are weighted with measured AODs so as to match the simulated total AOD with observation ($\sum_i \tau_i = \tau_{model} = \tau_{obs}$). Hereafter, the total AOD is referred to radiometer measurements, and AODs of aerosol constituents are weighted with observed AOD.

4 Estimation of DRE

The DRE of aerosols (natural and anthropogenic) is estimated as the difference in the solar radiative flux with and without the presence of aerosols in the atmosphere. The DRE is estimated at the top of the atmosphere (TOA), surface (SUR) and within the atmosphere (ATM) as

$$DRE_{TOA,SUR} = (F_{clean})_{TOA,SUR} - (F_{aerosol})_{TOA,SUR} \quad (4)$$

$$DRE_{ATM} = DRE_{TOA} - DRE_{SUR} \quad (5)$$

where F_{aero} and F_{clear} represent respectively the solar flux with and without the presence of aerosols in the atmosphere. From DRE_{ATM} , the diabatic heating rate ($\partial T/\partial t$) is estimated as

$$\frac{\partial T}{\partial t} = \frac{g}{C_p} \frac{DRE_{ATM}}{\Delta p} \quad (6)$$

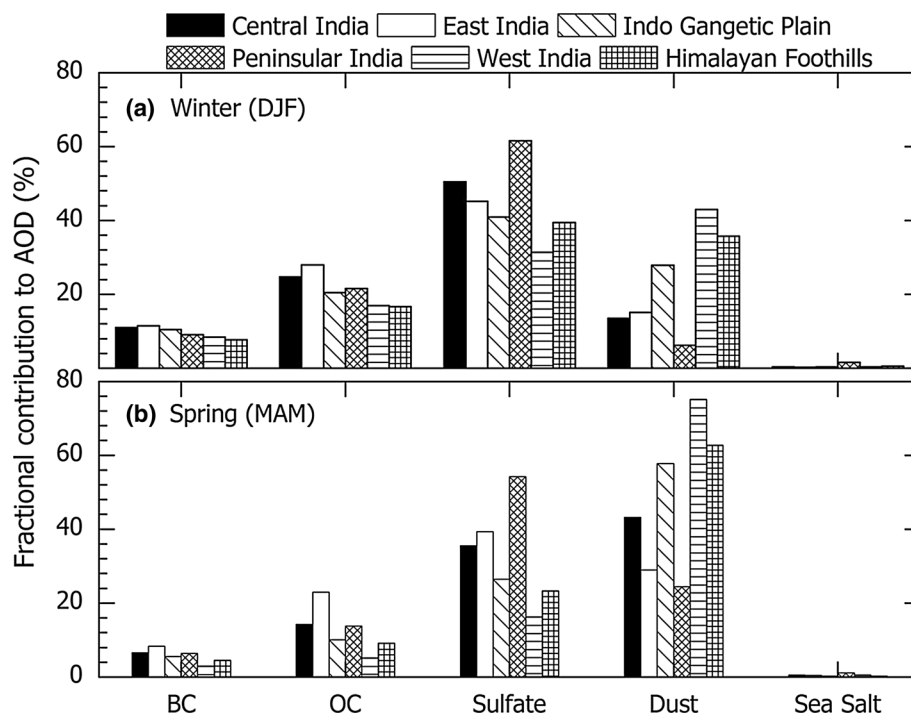
where g is the gravitational acceleration, C_p is the specific heat at constant pressure. The vertical extend of the atmosphere, which is influenced by the heating of aerosols, is denoted as Δp .

The Santa Barbara Discrete Ordinate Radiative Transfer (SBDART) model (Ricchiazzi et al. 1998) is used to simulate the radiative fluxes (F_{aero} and F_{clear}) at the top of the atmosphere and surface. The spectral AOD, SSA and asymmetry parameters along with the climatological seasonal values of columnar water vapor and ozone content and spectral variation of surface albedo are fed to the model for the simulation of radiative fluxes. In the case of composite aerosols, AOD, SSA and asymmetry parameter are taken from Eqs. 1, 2 and 3 as discussed above, whereas for the estimation of speciated DREs we have weighted the individual AODs (τ_i) with τ_{obs} and spectral variation of SSA and asymmetry parameter are taken from Hess et al. (1998). The meteorological and surface parameters needed for the estimation of DRE were taken from the long term satellite data. The seasonal mean values of columnar ozone and water vapor concentrations are taken respectively from the TOMS and MODIS (AQUA and TERRA) data, while MODIS land surface products are used for describing the spectral variation of surface albedo. These inputs are fed into the SBDART model to address the seasonal and spatial heterogeneity in the real atmosphere compared to the standard tropical atmosphere model and surface albedo provided in the radiative transfer model. The SBDART simulations were carried out for clear sky conditions at every half an hour interval from sunrise to sunset and then diurnally averaged. Hereafter the DRE described in this study is diurnally averaged for clear sky conditions, unless otherwise mentioned explicitly.

Based on the methodology discussed above, DREs have been estimated for the composite aerosols and its individual aerosol constituents. It should be noted that, even though the sum of all speciated AODs equals to the total measured AOD, the sum of the speciated DREs need not be same as that of DRE estimated for the composite aerosol system due to the multiple scattering and non-linearities involved in the aerosol–radiation interaction (Nair et al. 2014). This inherent uncertainty could lead to a difference of $\pm 10\%$ between the composite DRE and the sum of the individual constituents DRE. Nair et al. (2014) have discussed the sensitivity of speciated aerosol forcing to total aerosol loading, surface albedo and aerosol composition and have reported

Table 2 Seasonal mean aerosol optical depth at 500 nm over distinct locations over the Indian region

Region	Aerosol optical depth				
	Winter	Spring	Monsoon	Post monsoon	Annual
Peninsular India	0.42 ± 0.08	0.46 ± 0.08	0.39 ± 0.15	0.42 ± 0.09	0.43 ± 0.10
Central India	0.54 ± 0.09	0.52 ± 0.07	0.47 ± 0.11	0.49 ± 0.09	0.51 ± 0.07
IGP	0.63 ± 0.16	0.53 ± 0.1	0.68 ± 0.18	0.65 ± 0.21	0.63 ± 0.17
Western India	0.35 ± 0.05	0.40 ± 0.06	0.49 ± 0.10	0.42 ± 0.03	0.41 ± 0.08
Eastern India	0.63 ± 0.27	0.73 ± 0.24	0.49 ± 0.22	0.47 ± 0.18	0.58 ± 0.23
Islands	0.34 ± 0.02	0.35 ± 0.01	0.26 ± 0.14	0.30 ± 0.04	0.32 ± 0.07

Fig. 4 Fractional contribution of individual aerosol constituents to the aerosol optical depth during winter and spring seasons

that the non-linear effects of multiple scattering on constituents' DRE are very high over ocean surface than that over land. The sum of speciated DREs by considering only one aerosol species in atmosphere will overestimate the total DRE, whereas incorporating the effects of neighboring aerosol species on the speciated DRE would underestimate the total DRE. Hence, we have normalized the speciated DREs with total DRE, so that sum of constituent DREs will equal the composite DRE estimated using total AOD.

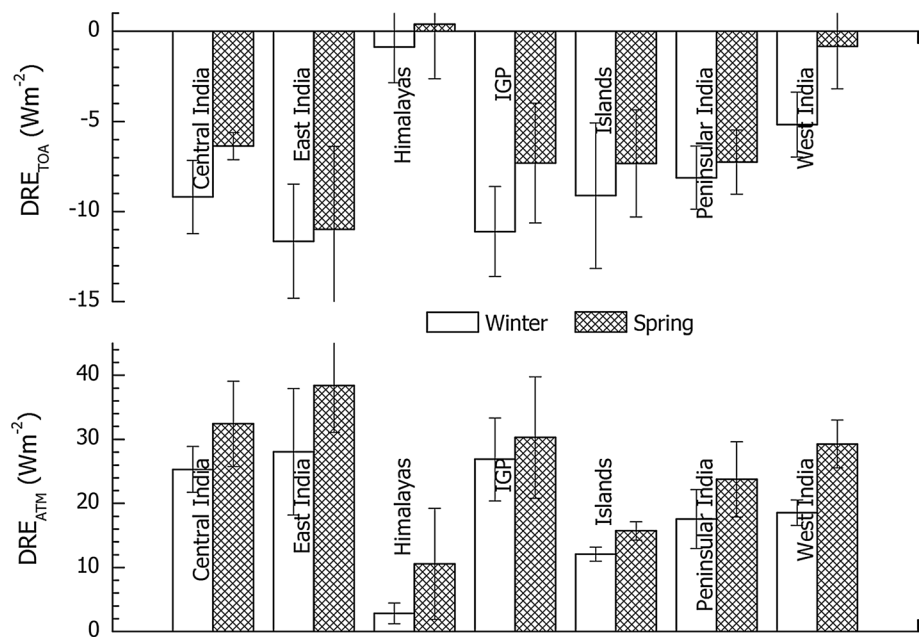
5 Results and discussions

5.1 Aerosol characteristics over India

Regional characteristics of AODs and their seasonality (over the Indian subcontinent) have been examined using the radiometer network data (ARFINET, AERONET, IMD) supplemented with GOCART model simulations.

The annual mean value of regionally averaged AOD at 500 nm over Indian region is 0.45 ± 0.2 . The annual mean values for different regions of Indian sub-continent such as, IGP, Eastern India, peninsular India and Western India are 0.63 ± 0.17 , 0.58 ± 0.23 , 0.43 ± 0.1 and 0.41 ± 0.1 respectively. Most of the Indian regions experience high aerosol load throughout the year as seen Table 2. The AOD at 500 nm over peninsular India varies from 0.42 ± 0.1 during winter (December to February) to 0.48 ± 0.08 during spring (March to May) and 0.39 ± 0.15 during summer (June to September) and 0.42 ± 0.09 during post-monsoon (October to November) seasons. The average fractional contribution of BC, OC, sulfate, dust and sea salt to the total AOD ($\tau_i \times 100/\tau_{\text{obs}}$) for 35 network observatories during winter and spring seasons are shown in Fig. 4. The summer monsoon and post-monsoon values are not included in the figure, in fact the fractional distribution of post-monsoon is more or less close to the winter pattern and summer monsoon values are similar to that of spring except an

Fig. 5 Direct radiative effects (DRE) due to composite aerosols at the top of the atmosphere (TOA) and within the atmosphere (ATM) over the distinct environments over the Indian subcontinent



increase in sea-salt and sulfate fraction and corresponding decrease in dust loading. In addition, summer monsoon measurements are sparse and values are sometimes contaminated due to very thin and moving clouds. The BC aerosols contributed $\sim 9.7 \pm 1.5$ % to total AOD during winter and 5.7 ± 1.8 % during spring season. The major contributor to the total AOD during winter is sulfate aerosols (44.8 ± 10.4 %), whereas mineral dust (48.7 ± 19.9 %) dominates during spring. The contribution of OC to the total AOD decreases from 21.4 ± 4 % in winter to 12.6 ± 6 % in spring. During summer monsoon period the fractional contribution of BC, OC, sulfate, dust and sea salt are 5.6 ± 1.1 , 11.6 ± 2.4 , 49.8 ± 6.4 , 28.2 ± 9.3 and 4.8 ± 2.9 % respectively. The highest contribution of OC to the total is observed over the East India, where biomass burning activities are significant during winter and spring seasons (Wang et al. 2007). However, the fractional contribution of BC remains ≤ 10 % (comparable to the standard deviations of dust and sulfate aerosol fraction) during both the seasons. Averaged over the Indian landmass, sea salt aerosols contribute less than one percent (~ 0.5 %) to the total AOD during winter and spring seasons; but as much as 5.5 % during summer monsoon period. However, sea-salt fraction could be significantly higher over the coastal region, especially during summer monsoon season. In general, anthropogenic aerosols dominated during winter and natural aerosols dominated during spring, which is mostly associated with the transition of synoptic scale monsoon circulations. Absorption aerosol optical depth (AAOD) at 500 nm simulated using GOCART model shows higher or similar values during spring than winter, irrespective of the decrease in BC fraction during spring. Hence the increase

in AAOD during spring is mostly attributed to the increase in dust loading during spring. The annual mean AAOD over the entire region is 0.051 ± 0.025 , and is about ~ 11 % of the AOD.

The fractional contribution of optical depth of BC to the total AOD observed over the Indian region matches well with the earlier reports by Ramanathan et al. (2001). These authors synthesized the aerosol measurements during Indian Ocean Experiment (INDOEX) over the northern equatorial Indian Ocean and reported ~ 10 % contribution from BC to the total. In contrast to the near surface aerosol concentrations, which decreases from winter to spring, the columnar aerosol loading remained same throughout the year with a slight increase during spring. This is inline with the recent aircraft experiments carried out over the Indian region as a part of Regional Aerosol Warming Experiment (RAWEX) during spring and winter (Babu et al. 2016). Examining the seasonality of the dominant source contributions to the columnar AOD and its spectral dependence, Beegum et al. (2008) have pointed out a transformation from the water soluble aerosol-dominated system in winter to dust dominated system in spring, especially over most of the Indian mainland. Climate implications of these two different aerosol regimes are yet to be quantified accurately. It should be noted that INDOEX focused more on the anthropogenic aerosols from the Indian region advected over to the Indian ocean during winter (Ramanathan et al. 2001) whereas the Integrated Campaign for Aerosols, gases and Radiation Budget (ICARB) focused on the transition from anthropogenic dominance to natural aerosol dominance during spring season (Moorthy et al. 2009).

Table 3 Regional mean values of DRE at TOA and heating rate during winter and spring seasons

Region	DRE _{TOA} (W m ⁻²)		Heating rate (K day ⁻¹)	
	Spring	Winter	Spring	Winter
Peninsular India	-7.3	-8.1	0.67	0.49
Central India	-6.4	-9.2	0.91	0.71
IGP	-7.3	-11.1	0.85	0.75
Western India	-0.8	-5.2	0.82	0.52
Eastern India	-11.0	-11.6	1.08	0.79
Himalayan Foothills	-7.9	-7.8	0.58	0.31
Himalayas	0.4	-0.9	0.30	0.08
Islands	-7.3	-9.1	0.44	0.34

5.2 Direct radiative effects over India

The regional variations of direct radiative effect (DRE) due to composite aerosols (natural and anthropogenic) at the TOA and within the atmosphere for winter and spring over various regions of the Indian subcontinent are shown in Fig. 5. The regional mean DREs for the entire Indian subcontinent at TOA, surface and atmosphere are -8.6 ± 3 , -28.2 ± 12 , and 19.6 ± 9 W m⁻² respectively during winter and -6.8 ± 4 , -33.7 ± 12 and 26.9 ± 9 W m⁻² during spring. Compared to winter, higher warming occurs at the TOA and within the atmosphere during spring season.

This clearly indicates that the aerosol system over Indian region is more absorptive during spring and produces more warming in the atmosphere than during winter. Examining sub-regionally, the magnitudes of DRE_{TOA} and DRE_{ATM} are higher over Eastern India and IGP followed by central and peninsular India. More than 25 W m⁻² of solar radiation is being trapped in the atmosphere by the aerosols over East India, IGP and Central India during both the seasons. It is interesting to note that, far away from the continental sources, the DREs over the oceans around India are not very low because of the transport of natural and anthropogenic aerosols from the landmasses to the oceans. Regional mean values of heating rate due to aerosols during winter and spring seasons are given in Table 3. The diabatic heating rates estimated from the DRE_{ATM} shows highest value of 1 K day⁻¹ over the Eastern India and lowest value of 0.67 K day⁻¹ over peninsular India during spring. Except at the Himalayan and Island stations, the heating rate values are higher than 0.5 K day⁻¹ during spring and winter indicating the importance of diabatic heating of aerosols on regional climate.

Several studies have compiled the radiative forcing values from distinct locations over the Indian region (Babu et al. 2002; Ganguly and Jayaraman 2006; Dey and Tripathi 2008; Pathak et al. 2010). All the studies have unambiguously reported significant surface cooling and atmospheric warming due to aerosols over the region. However, the TOA DREs reported by several authors indicate large

Table 4 Direct radiative effects (DRE) at TOA and atmosphere at different locations

Location	DRE _{TOA} (W m ⁻²)	DRE _{ATM} (W m ⁻²)	Period	SSA	Technique	References
Jaipur	-5.3 ± 2.0	26.2 ± 5.0	Annual	0.902 ± 0.026	AERONET	Present study
Pune	-7.3 ± 1.5	22.4 ± 3.7		0.879 ± 0.026		
Kanpur	-6.9 ± 2.4	33.9 ± 6.2		0.887 ± 0.028		
Gandhi College	-8.2 ± 1.9	32.3 ± 6.7		0.899 ± 0.032		
Ranichauri	-10.9 ± 2.5	16.0 ± 8.3	Annual	0.904 ± 0.017	IMD Sky-net	Present study
Rohtak	-12.2 ± 2.7	20.1 ± 4.4		0.913 ± 0.021		Soni et al. (2014)
Guwahati	-15.0 ± 3.6	31.6 ± 12.1		0.904 ± 0.015		
Varanasi	-14.0 ± 1.1	35.5 ± 5.9		0.905 ± 0.020		
Bangalore	+5.0	+28.0	Oct–dec, 2001	0.73	Semi empirical	Babu et al. (2002)
Dibrugarh	-1.4 ± 2.9	35.7 ± 6.4	Pre monsoon	~0.8		Pathak et al. (2010)
Nainital	+0.7	4.9	December 2004	0.90 ± 0.03		Pant et al. (2006)
Ahmedabad	0–4	45–60	Winter	0.68 ± 0.04		Ramachandran and Kedia (2010)
	-7 to 0	20–44	Spring	0.83 ± 0.08		
Trivandrum	1.8–4.1	46.6–52.9	Winter	0.7–0.74		Babu et al. (2007)
	-1.4 to 0.3	32.8–37.6	Spring	0.78–0.81		
Kanpur	-13 ± 3	30	Winter	0.92 ± 0.02	Measured aerosol chemistry	Dey and Tripathi (2007)
Ahmedabad			Winter	0.73 ± 0.10	Ground based in situ	Ganguly et al. (2006)
			Spring	0.84 ± 0.04		

The corresponding aerosol single scattering albedo is also shown in the table

heterogeneity, not only in the magnitude but also the sign of the DRE (Table 4). In the present study, TOA DRE over Indian region is found to range from -8.6 to -6.8 W m^{-2} , which indicates significant cooling due to aerosols at TOA. The difference in TOA DRE between the earlier studies and present work is mostly attributed to the relatively lower SSA values estimated by the previous studies using a semi empirical hybrid approach (Table 4). In this method, measured values of spectral AOD and black carbon mass concentration at the surface level are used as constraints to estimate the single scattering albedo and asymmetry parameter by assuming an aerosol chemical model of Hess et al. (1998), which reproduces the measured aerosol properties accurately (Satheesh and Srinivasan 2006). The SSA values reported by the semi-empirical techniques are systematically lower than the SSA values retrieved using the AERONET and IMD radiometers at various locations (Table 4).

Surface albedo is another critical parameter, which influences the magnitude and sign of the aerosol forcing significantly. Haywood and Shine (1995) have shown that aerosol albedo higher than the critical single scattering albedo (which is a function of surface albedo and aerosol backscatter fraction) cools the TOA and aerosol SSA lower than the critical SSA induces warming at the TOA. This implies that aerosol SSA should be sufficiently lower (<0.8) to warm the TOA over the ocean, whereas small fraction of absorbing aerosols makes TOA warming over the snow/ice surfaces. Generally, this transition from warming to cooling occurs around an aerosol albedo of 0.85 over the land surface. McComiskey et al. (2008) have clearly showed that aerosol DRE at the TOA and surface becomes more positive as the surface albedo increases. The range of critical SSA for a vegetated land surface (0.15–0.2) and aerosol upscatter fraction of 0.1–0.2 is estimated as 0.675–0.862. The upper bound of the critical single scattering albedo is lower than the mean SSA reported in this study (0.886 ± 0.03). In general, aerosol SSA measured by radiometers (AERONET/IMD) reported higher values than the critical SSA, whereas in situ measurements (ground level) and semi-empirical approach reported lower SSA than the critical SSA. The major challenge in the accurate estimation of aerosol radiative forcing at the top of the atmosphere is mostly associated with the uncertainties in the SSA values.

Based on the ICARB observations over the oceans around the Indian subcontinent, Moorthy et al. (2009) and Nair et al. (2013b) have reported a warming of 0.3 – 0.9 K day^{-1} in the lower free troposphere during spring season, whereas several other studies reported significantly higher heating rates over the Indian landmass (Dey and Tripathi 2008; Satheesh et al. 2008; Pathak et al. 2010). In the backdrop of the seasonal transformation of the vertical

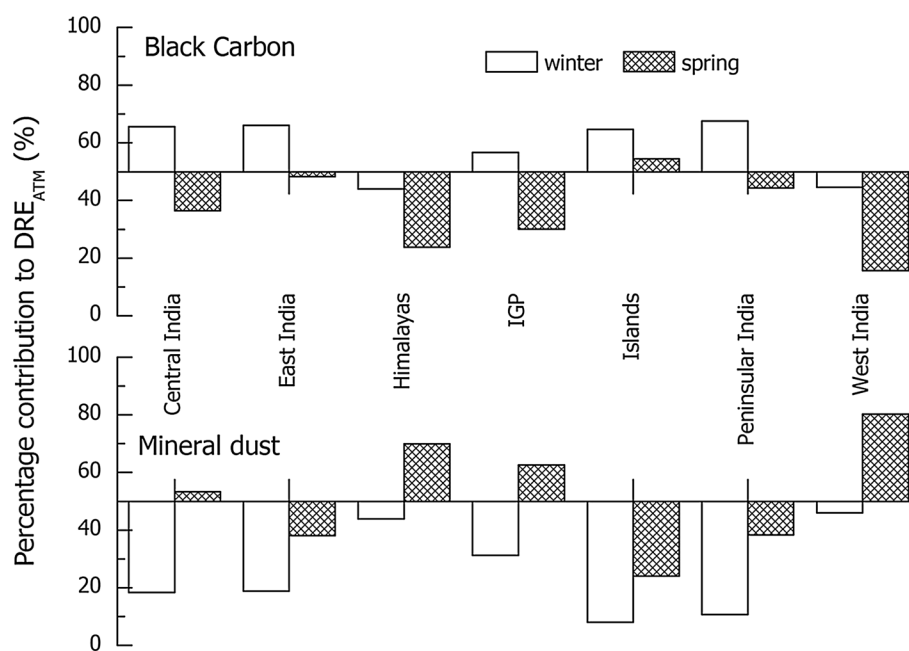
distribution of aerosols from winter to spring, aerosol induced diabatic heating is more important in the boundary layer during winter and it can be distributed to as high as 6–10 km during spring season. Based on aircraft measurements, Babu et al. (2016) have reported that springtime aerosols are more absorptive in nature (low columnar SSA) and spring time aerosol loading in the lower free troposphere ($<3 \text{ km}$) is almost 10 to 20 times higher than that in winter. During winter, aerosols are mostly confined within the boundary layer and consequently there exists a significant vertical gradient in the aerosol-induced diabatic heating. This would modify the lapse rate, especially over the IGP and Eastern India. In contrast to winter, aerosols are lofted high in the atmosphere (up to 6–10 km) during spring and heating rate values, though smaller at lower altitudes (compared to winter), continue to contribute steadily up to mid/upper free troposphere, where the lower air density is conducive for larger heating.

5.3 Absorbing aerosols: BC versus dust

Absorbing aerosols are important in as much as they produce significant greenhouse warming in the atmosphere. We have estimated the speciated DREs for BC and dust as mentioned in Sect. 4. Figure 6 shows the regional characteristics of percentage contribution of these two major absorbing species (BC and dust) to the total DRE_{ATM} over the Indian region during spring and winter. It is seen that BC aerosols contribute more than 50 % to the DRE_{ATM} during winter over most of the Indian stations except over the Himalayas and Western India, where BC contributes around 40 %. This role is taken over by dust aerosols during spring, which contribute more than 50 % of the DRE_{ATM} over central India, Himalayas, IGP and Western India, and ~ 40 % over the rest of the region, except over the islands. During spring season, the impact of BC is highly reduced in contrast to winter. This pattern reveals an interesting transformation of the aerosol types that heat the atmosphere; with BC being the major player in winter and mineral dust in spring. The magnitude of the diabatic heating are comparable or slightly higher during spring over most of the regions (Table 3; Fig. 5 and Sect. 5.2), in fact the dominant absorbing aerosol species changed from anthropogenic (BC) to natural (dust). While BC contributed 56 % of DRE_{ATM} during winter, dust contributed to 62 % during spring.

Absorbing aerosols over South Asia continue to be the focus of scientific discussion because of their significant dominance in total aerosol load and implications for the regional climate (Menon et al. 2002; Ramanathan et al. 2005; Wang et al. 2007; Meehl et al. 2008; Vinoj et al. 2014). The influence of free tropospheric aerosol absorption on the early onset of monsoon over the Himalayan

Fig. 6 Percentage contribution of black carbon and dust aerosols to the direct radiative effects within the atmosphere (DRE_{ATM}) over the distinctly different regions during winter and spring seasons



foothills (Lau et al. 2006) and dynamical coupling of dust forcing on Indian monsoon characteristics (Vinoj et al. 2014) highlight the importance of aerosol absorption on the Indian monsoon. Chung and Zhang (2004) have shown that elevated aerosols above the boundary layer have significant influence on the surface temperature and vertical profiles of diabatic heating rate due to which, the aerosols affect the precipitation pattern significantly over the Indian region (Ramanathan et al. 2005). Vinoj et al. (2014) have reported that the short period variabilities of dust sources influence the Indian monsoon by atmospheric responses due to dust induced diabatic heating and changing the large scale circulation. Using a coupled ocean–atmosphere model, Bollasina et al. (2011) attributed the decreasing trend in Indian summer monsoon rainfall to the dynamical feedback of anthropogenic aerosols. In the absence of anthropogenic BC aerosols (before industrial revolution), aerosol induced diabatic heating might have followed the seasonal variations of the natural dust; winter minimum and high during spring and summer. Hence the recent increase in the emission of BC aerosols reduced the seasonal asymmetry in the aerosol induced diabatic heating in the atmosphere.

5.4 Carbonaceous and anthropogenic aerosol effects/forcings

The anthropogenic DRE or direct radiative forcing (DRF) is estimated from two additional simulations of GOCART; first with all the aerosol sources (ALL) and then with natural sources (NAT) of BC, OC and sulfates. We have considered dust and sea salt as completely natural. The fractional contribution of anthropogenic sources to the AODs of BC,

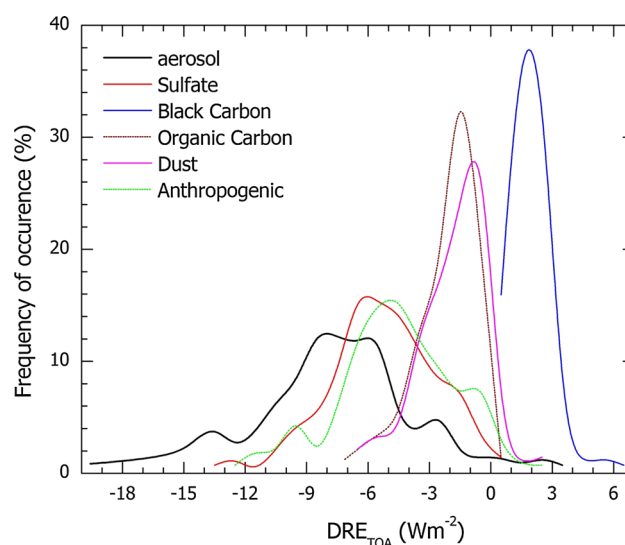


Fig. 7 Frequency of occurrence of the direct radiative effects at the top of the atmosphere (DRE_{TOA}) due to various aerosol constituents, total and anthropogenic aerosols for all months over the entire Indian region

OC and sulfate is estimated as $1-(NAT/ALL)$. Frequency of occurrence of DREs at TOA over the Indian region, due to different aerosol species, total composite aerosols and anthropogenic aerosols is shown in Fig. 7. The width of the frequency distribution implies the spatio-temporal heterogeneities in the characteristics of composite and individual aerosol species over the region. The BC depicts narrow distribution with a mean value of $1.9 \pm 1 \text{ W m}^{-2}$ in contrast to relatively broad distribution of total, anthropogenic and sulfate aerosols. The OC and dust have similar frequency

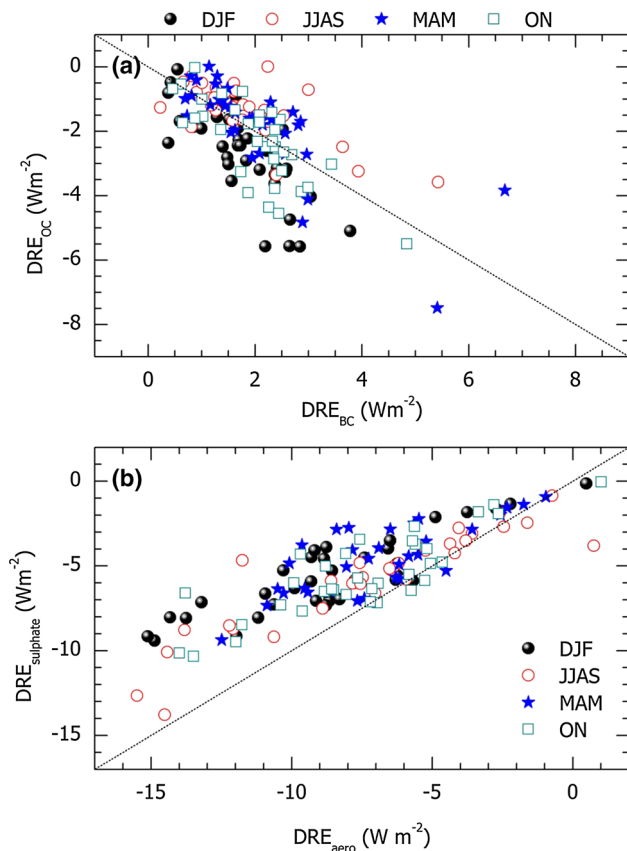


Fig. 8 Scatter diagram of direct radiative effect due to **a** black carbon and organic carbon and **b** sulfate aerosols and composite aerosols over the Indian region. Seasons are depicted with separate *symbols*

distributions with annual mean value for TOA effect is respectively, -2.06 ± 1.4 and $-1.8 \pm 1.7 \text{ W m}^{-2}$. As seen in the figure, the mean values of DRE_{TOA} for BC and OC have comparable magnitudes but have opposite sign. The sulfate aerosols ($-5.3 \pm 2.6 \text{ W m}^{-2}$) contribute more than 71 % to the total DRE. Interestingly, sulfate and anthropogenic DRE followed the similar broad distribution, indicating the large spatio-temporal heterogeneity.

Figure 8 shows the scatter diagram of DRE at TOA due to BC versus OC during four seasons. It is interesting to note that, in general, the warming due to BC at the TOA is compensated fully or even slightly overwhelmed by the cooling due to OC at TOA, in all the seasons; with a large variability. The sum of the DRE_{TOA} due to BC and OC is $-0.13 \pm 1 \text{ W m}^{-2}$, which indicates a small net cooling at TOA due to carbonaceous aerosols (BC + OC). This amounts to only less than 2 % of the total aerosol DRE. It should be noted that, at low values of BC DRE, the net effect is warming at TOA and for the higher values of BC DRE, TOA cools due to the dominance of OC DRE over the warming due to BC. It is interesting to note that the magnitude of the TOA effect due to these two species (OC

and BC) are comparable, despite OC contributes twice as much to AOD as BC. In contrast to DRE at TOA, atmospheric warming due to BC ($\sim 10.5 \text{ W m}^{-2}$) is much higher than OC ($\sim 0.85 \text{ W m}^{-2}$) and are additive in nature. The scatter diagram of DRE_{TOA} for sulfate versus total aerosols for different seasons is shown in the bottom panel of Fig. 8. It is seen that, most of the values occur close to or above the 1:1 line, which indicates that the DRE due to sulfate is the prime contributor to the total DRE at TOA. Due to the compensation effect of DRE due to BC and OC at TOA, sulfate aerosols dominate (71 %) the total aerosol DRE. This effect is stronger during summer monsoons and post monsoon periods. This clearly indicate that, to estimate an accurate DRE over India, sulfate measurements have to be constrained properly with multi-platform measurements and modeling.

In general, BC and OC are mostly co-emitted; only their ratios vary depending on the source characteristics. Consequently, any mitigation of BC would result in reduction of OC also, and in the light of the findings discussed just above (that at lower forcing, BC forcing dominates over OC) the net effect would be determined more by the BC concentration. This falls in line with the reported warming of the atmosphere, associated with reduction of BC reported by Novakov et al. (2008). Wang et al. (2007) have also reported that the radiative forcings of BC aerosols emitted from the biomass burning are overshadowed by the OC at the top of the atmosphere. It, thus, clearly emerges that as far as the radiative perturbations are considered BC–OC aerosol system have less forcing at TOA, than a less OC aerosol system or a no-OC or only BC aerosol system. Whereas the atmospheric radiative effect due to BC and OC are additive and internal mixture of BC and OC are more absorptive than their external mixture. In general, the low values of BC are associated with fossil fuel burning and high BC values are often seen during biomass burning events. On the backdrop of all these, it appears that fossil fuel aerosols (BC and OC) have more net warming effect (at TOA and in the atmosphere) than their biomass burning counterparts, which have net cooling (though very small) at the TOA. Hence, an ideal mitigation strategy of decreasing BC alone would increase the cooling at TOA whereas decrease in BC and OC together (realistic strategy) would result in decrease in cooling at TOA.

5.5 Gradients in anthropogenic DRE

The fractional contribution of anthropogenic aerosols to the total DRE at TOA is estimated as described above and its latitudinal gradient is shown in Fig. 9. Interestingly, and in contrast to the general belief, the anthropogenic fraction decreased from south to north, which indicates that the ‘high aerosol load’ over the northern Indian region

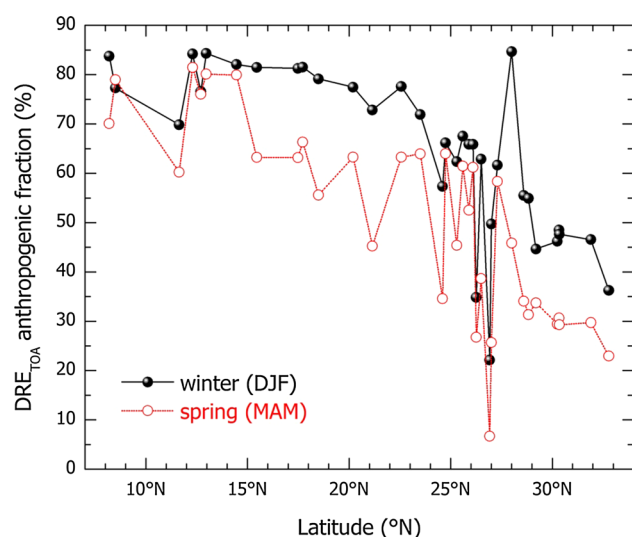


Fig. 9 Latitudinal gradients in the fractional contribution of anthropogenic aerosols to the total direct radiative forcings at top of the atmosphere during winter and spring seasons

has relatively higher natural aerosol fraction than that in the southern parts of India. During winter, the anthropogenic fraction of DRE decreases from 80 % over southern India to 40 % over North, where as significant reduction in anthropogenic fraction is observed during spring over north India. Even though the aerosol concentration over the southern peninsula is lower than that over other parts of the country, it seems to be dominated by anthropogenic aerosol species. During INDOEX, Ramanathan et al. (2001) have reported $\sim 80 \pm 10$ % of anthropogenic aerosol contribution to the total AOD over the northern Indian Ocean; which again is in conformity to the inferences in this study. Based on the shipborne and satellite measurements supplemented with chemical transport model simulations, Nair et al. (2010) have reported that the anthropogenic fraction over the Bay of Bengal has an opposite gradient to that of aerosols loading. These authors confirmed that the so called pristine regions of the southern Bay of Bengal have higher anthropogenic fraction than northern Bay of Bengal, despite of it being closer to all the anthropogenic sources and immediately affected by the IGP outflow. Synthesizing measurements during a mobile land campaign over southern peninsular India during winter 2004, Moorthy et al. (2007) have reported a decrease in BC mass fraction from South to North which also lends further support the high anthropogenic fraction in the southern peninsula.

Latitudinal gradients in DRE_{ATM} due to BC, dust and total aerosols during spring and winter seasons over the Indian mainland are shown in Fig. 10. In general, a three-fold increase in aerosol absorption is observed from south to north and higher values are observed during spring compared to the winter. Interestingly, DRE due to BC doesn't

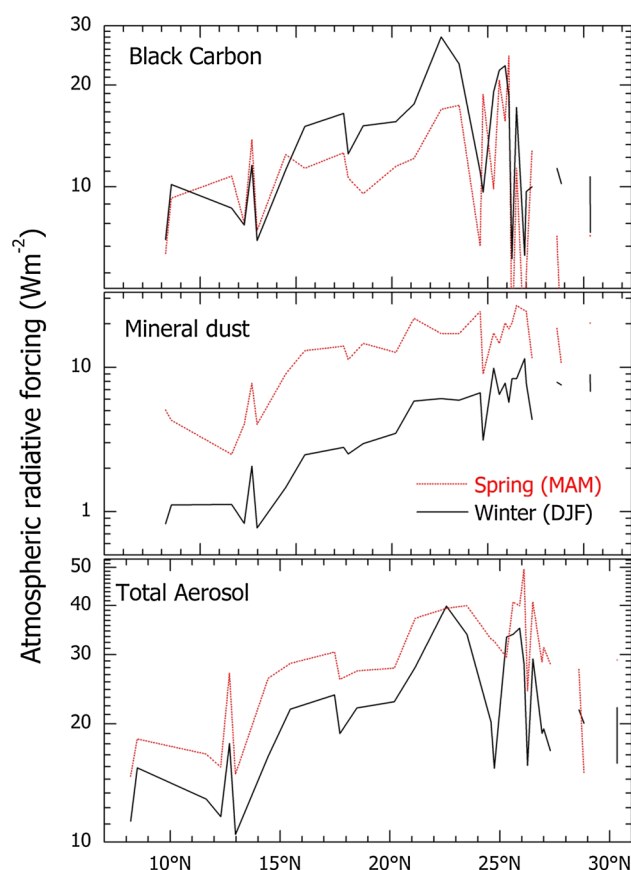


Fig. 10 Latitudinal gradients in the atmospheric radiative effects due to black carbon, dust and total aerosols during spring and winter season over the Indian region

show much seasonal variation except over central India. DRE_{ATM} due to BC varied from $\sim 10 \text{ W m}^{-2}$ at 7°N to $\sim 20 \text{ W m}^{-2}$ at 27°N . In contrast to BC, DRE due to dust aerosols shows significant seasonal variations with spring high and summer low. Compared to BC aerosols, mineral dust depict large gradient in atmospheric DRE along the latitudes especially during spring season. During spring, DRE varied from 4 W m^{-2} at 7°N to $\sim 20 \text{ W m}^{-2}$ at 27°N . Combining the absorption due to BC and mineral dust, total aerosols also show significant latitudinal gradient; low DRE values at south and high values at north. These north south gradients in aerosol properties and radiative forcings are the characteristics of this region. It may also be noted that based on airborne measurements of aerosol extinction during ICARB, Satheesh et al. (2008) have reported a northward meridional gradient in aerosol induced atmospheric heating rate and the position of the peak heating during spring.

In the present study, the seasonal mean gradients were estimated for 8°N – 30°N over the Indian landmass using a network of ground based observatories and aerosol modeling. Earlier studies onboard ship and aircraft have also shown significant gradients in the zonal and meridional

directions (Nair et al. 2013b). Similar gradients were observed over the ocean around Indian peninsula using extensive shipborne measurements (Ramanathan et al. 2001; Nair et al. 2010) and long-term satellite measurements (Satheesh et al. 2006). The gradient in atmospheric DRE is a persistent feature over the Indian region. Both natural (dust) and anthropogenic (BC) aerosols show meridional gradient during spring and winter. The anthropogenic activities during the last few decades strengthened the magnitude of DRE, especially atmospheric absorption due to BC, during winter; hence the gradients in both winter and spring are almost similar in magnitude. The implication of this change in DRE gradient has to be explored in the context of aerosol–monsoon interaction over the Indian region using coupled ocean atmosphere model simulations. The role of anthropogenic aerosols on the wintertime atmospheric stability and boundary layer thermodynamics needs to be investigated on the backdrop of ‘dome effect’ suggested by Ding et al. (2016) over East Asia.

Present study shows a significant forcing due to anthropogenic aerosols over the Indian region. Direct and indirect radiative effects of anthropogenic and natural aerosols induce significant effect on atmospheric dynamics and hydrological cycle. Wang et al. (2015) have reported that elevated aerosol pollution over South Asia lead to the surface cooling by 0.1 K and weakening of northern branch of Hadley cell in an Asian aerosol only scenario. Several studies have shown that diabatic heating of aerosols in the atmosphere leads to non-local and fast responses in the atmospheric circulation and moisture convergence, thereby affecting the aerosol–monsoon interaction over the region (Ganguly et al. 2012; Vinoj et al. 2014; Lau 2016). Based on a coupled ocean atmosphere modeling framework, Bollasina et al. (2011) have attributed the radiative effects of anthropogenic aerosols as the major reason for the drying signal seen over the Central India during the present decade. These authors have reported the weakening of tropical meridional circulation due to aerosols. An association between the absorption aerosol optical depths with ENSO (El-Nino Southern Oscillation) reported by Kim et al. (2015) highlighted the amplification of ENSO signal by absorbing aerosols during the La Nina years in comparison to the normal La Nina years. In the present study we have shown that aerosol induced diabatic heating and its meridional gradients are significantly high during spring and winter, indicating a potential forcing/driver on regional hydroclimate. Based on a coupled ocean–atmosphere model simulation, D’Errico et al. (2015) have suggested that the ‘local distribution and time of the season of the aerosol loading’ are important in understanding the aerosol effect on monsoon rainfall and its intrinsic variabilities. However, to understand the implications of South Asian aerosols on atmospheric dynamics and the variabilities of monsoon

rainfall, a systematic approach which involve coupled earth-system modeling and long-term measurements are essential to unravel the complex pathways of aerosol monsoon interactions (Lau 2016).

6 Conclusions

The comprehensive and extensive compilation of the aerosol measurements over the Indian region has been carried out for the first time using the data collected from the 35 ground based observatories spread across the Indian region. These measurements were supplemented with GOCART model simulations to estimate the seasonal variations in direct radiative effects of aerosol constituents, total and anthropogenic aerosols.

- In general, aerosol optical depth doesn’t show significant seasonal variations over the Indian region. However aerosol chemical composition significantly changes with season. A systematic transformation of anthropogenic to natural aerosol system has been observed over the Indian region as season progressed from winter to spring.
- Atmospheric warming due to aerosols are higher over central India, Indo Gangetic Plain and east India compared to the moderate values seen over peninsular, west India and over island locations. However, atmospheric warming due to BC aerosols contributes more than 60 % of the total warming during winter except over Himalayas and west India; whereas it reduces to ~35 % during spring over central, west, IGP and Himalayas.
- The large spread in the monthly mean DRE values estimated over the region is mostly attributed to the spread in the sulfate aerosol forcing (so anthropogenic aerosols) rather than due to BC and OC.
- The net forcing due to carbonaceous aerosols (BC + OC) at the top of the atmosphere is slightly negative or close to zero (with a large standard deviation) since magnitude of BC and OC DREs are similar and opposite in sign. This indicates that warming due to BC at TOA is fully compensated or overwhelmed by the cooling effect due to OC aerosols. Hence, the TOA forcing due to anthropogenic aerosols is mostly contributed by sulfate aerosols, since the contribution of BC and OC balances with a small cooling at TOA.
- The aerosols over the Indian region depict significant latitudinal gradients in aerosols loading and DRE from south to north. Even though high aerosol optical depth values are seen over the northern parts of the country, contribution of anthropogenic aerosols to the total decreases towards north high (almost 80 %) values over the southern peninsula. The magnitude of the latitudinal

gradients in the DRE due to dust aerosols increases significantly from winter to spring. This clearly indicates the importance of dust aerosols over the Indian region during pre-monsoon season.

Acknowledgments This study has been carried out as a part of ARFI project of the ISRO-Geosphere Biosphere program. We thank the seamless effort made by the each and every ARFINET PIs for their interest and dedication to support the program, which resulted in such long term aerosol data over the region. Details of ARFINET are available at: <http://spl.gov.in>. We also acknowledge NASA AERONET and IMD for providing aerosol data over the Indian region. The authors acknowledge the NASA Giovanni for GOCART data, MODIS and TOMS data made available.

Compliance with ethical standards

Conflict of interest The authors declare that they have no conflict of interest.

References

- Ackerman AS, Toon OB, Stevens DE, Heymsfield AJ, Ramanathan V, Welton EJ (2000) Reduction of tropical cloudiness by soot. *Science* 288:1042–1047
- Babu SS, Satheesh SK, Moorthy KK (2002) Aerosol radiative forcing due to enhanced black carbon at an urban site in India. *Geophys Res Lett* 29(18):1880. doi:[10.1029/2002GL015826](https://doi.org/10.1029/2002GL015826)
- Babu SS, Moorthy KK, Satheesh SK (2007) Temporal heterogeneity in aerosol characteristics and the resulting radiative impacts at a tropical coastal station—Part 2: direct short wave radiative forcing. *Ann Geophys* 25:2309–2320
- Babu SS, Manoj MR, Moorthy KK, Gogoi MM, Nair VS, Kompalli SK, Satheesh SK, Niranjana K, Gopal R, Bhuyan PK, Singh D (2013) Trends in aerosol optical depth over Indian region: potential causes and impact indicators. *J Geophys Res Atmos* 118:11794–11806. doi:[10.1002/2013JD020507](https://doi.org/10.1002/2013JD020507)
- Babu SS, Nair VS, Gogoi MM, Moorthy KK (2016) Seasonal variation of vertical distribution of aerosol single scattering albedo over Indian sub-continent: RAWEX aircraft observations. *Atmos Environ* 125:312–323
- Beegum SN, Moorthy KK, Nair VS, Babu SS, Satheesh SK, Vinoy V, Reddy RR, Gopal KR, Badarinarath KVS, Niranjana K, Pandey SK, Behera M, Jeyaram A, Bhuyan PK, Gogoi MM, Singh S, Pant P, Dumka UC, Kant Y, Kuniyal JC, Singh D (2008) Characteristics of spectral aerosol optical depths over India during ICARB. *J Earth Syst Sci* 117(S1):303–313
- Bollasina M, Ming Y, Ramaswamy V (2011) Anthropogenic aerosols and the weakening of the South Asian summer monsoon. *Science* 334:502–505. doi:[10.1126/science.1204994](https://doi.org/10.1126/science.1204994)
- Chin M, Ginoux P, Kinne S, Torres O, Holben BN, Duncan BN, Martin RV, Logan JA, Higurashi A, Nakajima T (2002) Tropospheric aerosol optical thickness from the GOCART model and comparisons with satellite and sunphotometer measurements. *J Atmos Sci* 59:461–483
- Chin M, Diehl T, Dubovik O, Eck TF, Holben BN, Sinyuk A, Streets DG (2009) Light absorption by pollution, dust, and biomass burning aerosols: a global model study and evaluation with AERONET measurements. *Ann Geophys* 27:3439–3464
- Chin M, Diehl T, Tan Q, Prospero JM, Kahn RA, Remer LA, Yu H, Sayer AM, Bian H, Geogdzhayev IV, Holben BN, Howell SG, Huebert BJ, Hsu NC, Kim D, Kucsera TL, Levy RC, Mishchenko MI, Pan X, Quinn PK, Schuster GL, Streets DG, Strode SA, Torres O, Zhao X-P (2014) Multi-decadal variations of atmospheric aerosols from 1980 to 2009: a perspective from observations and a global model. *Atmos Chem Phys* 14:3657–3690
- Chung CE, Zhang GJ (2004) Impact of absorbing aerosol on precipitation: dynamic aspects in association with convective available potential energy and convective parameterization closure and dependence on aerosol heating profile. *J Geophys Res* 109:D22103. doi:[10.1029/2004JD004726](https://doi.org/10.1029/2004JD004726)
- D’Errico M, Cagnazzo C, Gogli PG, Lau WKM, Hardenberg J, Fierli F, Cherchi A (2015) Indian monsoon and the elevated heat pump mechanism in a coupled aerosol-climate model. *J Geophys Res*. doi:[10.1002/2015JD023346](https://doi.org/10.1002/2015JD023346)
- Deepshikha S, Satheesh SK, Srinivasan J (2006) Dust aerosols over India and adjacent continents retrieved using METEOSAT infrared radiance Part II: quantification of wind dependence and estimation of radiative forcing. *Annales Geophysicae* 24(1):63–79
- Dey S, Tripathi SN (2007) Estimation of aerosol optical properties and radiative effects in the Ganga basin, northern India, during the wintertime. *J Geophys Res* 112:D03203
- Dey S, Tripathi SN (2008) Aerosol direct radiative effects over Kanpur in the Indo-Gangetic basin, northern India: long-term (2001–2005) observations and implications to regional climate. *J Geophys Res* 113:D04212. doi:[10.1029/2007JD009029](https://doi.org/10.1029/2007JD009029)
- Ding AJ, Huang X, Nie W, Sun JN, Kerminen V-M et al (2016) Enhanced haze pollution by black carbon in megacities in China. *Geophys Res Lett* 43:2873–2879. doi:[10.1002/2016GL067745](https://doi.org/10.1002/2016GL067745)
- Dubovik O, Smirnov A, Holben BN, King MD, Kaufman YJ, Eck TF, Slutsker I (2000) Accuracy assessment of aerosol optical properties retrieval from AERONET sun and sky radiance measurements. *J Geophys Res* 105:9791–9806
- Flanner MG, Zender CS, Randerson JT, Rasch PJ (2007) Present-day climate forcing and response from black carbon in snow. *J Geophys Res* 112:D11202. doi:[10.1029/2006JD008003](https://doi.org/10.1029/2006JD008003)
- Ganguly D, Jayaraman A (2006) Physical and optical properties of aerosols over an urban location in western India: implications for shortwave radiative forcing. *J Geophys Res* 111:D24207. doi:[10.1029/2006JD007393](https://doi.org/10.1029/2006JD007393)
- Ganguly D, Jayaraman A, Gadhave H (2006) Physical and optical properties of aerosols over an urban location in western India: seasonal variabilities. *J Geophys Res* 111:D24206
- Ganguly D, Rasch PJ, Wang H, Yoon J-H (2012) Climate response of the South Asian monsoon system to anthropogenic aerosols. *J Geophys Res* 117:D13209
- Hansen J, Sato M, Ruedy R, Nazarenko L et al (2005) Efficacy of climate forcings. *J Geophys Res* 110:D18104. doi:[10.1029/2005JD005776](https://doi.org/10.1029/2005JD005776)
- Haywood J, Boucher O (2000) Estimates of the direct and indirect radiative forcing due to tropospheric aerosols: a review. *Rev Geophys* 38(4):513–543
- Haywood JM, Shine KP (1995) The effect of anthropogenic sulfate and soot aerosol on the clear sky planetary radiation budget. *Geophys Res Lett* 22(5):603–606
- Hess M, Koepke P, Schult I (1998) Optical properties of aerosols and clouds: the software package OPAC. *Bull Am Meteorol Soc* 79:831–844
- Holben BN, Eck TF, Slutsker I, Tanre D et al (1998) AERONET—a federated instrument network and data archive for aerosol characterization. *Remote Sens Environ* 66:1–16
- Intergovernmental Panel on Climate Change (IPCC) (2007) Climate change 2007: the physical science basis. In: Solomon S, Qin D, Manning M, Chen Z, Marquis M, Averyt KB, Tignor M, Miller HL (eds) Contribution of working group I to the fourth assessment report of the IPCC. Cambridge University Press, Cambridge and New York

- Jethva H, Satheesh SK, Srinivasan J, Moorthy KK (2009) How good is the assumption about visible surface reflectance in MODIS aerosol retrieval over land? A comparison with aircraft measurements over an urban site in India. *IEEE Trans Geosci Remote Sens* 47:1990–1998. doi:[10.1109/TGRS.2008.2010221](https://doi.org/10.1109/TGRS.2008.2010221)
- Kaufman YJ, Boucher O, Tanre D, Chin M, Remer L, Takemura T (2005) Aerosol anthropogenic component estimated from satellite data. *Geophys Res Lett* 32:L17804. doi:[10.1029/2005GL023125](https://doi.org/10.1029/2005GL023125)
- Kim MK, Lau WKM, Kim K-M, Sang J, Kim Y-H, Lee W-S (2015) Amplification of ENSO effects on Indian summer monsoon by absorbing aerosols. *Clim Dyn*. doi:[10.1007/s00382-015-2722-y](https://doi.org/10.1007/s00382-015-2722-y)
- Kompalli SK, Babu SS, Moorthy KK (2010) Inter-comparison of aerosol optical depth from the multi-wavelength solar radiometer with other radiometric measurements. *Ind J Radio Space Phys* 39:364–371
- Lau WKM (2014) Desert dust and monsoon rainfall. *Nat Geosci* 7:255–256. doi:[10.1038/ngeo2115](https://doi.org/10.1038/ngeo2115)
- Lau WKM (2016) The aerosol-monsoon climate system of Asia: a new paradigm. *J Meteorol Res*. doi:[10.1007/s13351-015-5999-1](https://doi.org/10.1007/s13351-015-5999-1)
- Lau KM, Kim MK, Kim KM (2006) Asian summer monsoon anomalies induced by aerosol direct forcing: the role of the Tibetan Plateau. *Clim Dyn* 26:855–864
- Lawrence MG, Lelieveld J (2010) Atmospheric pollutant outflow from southern Asia: a review. *Atmos Chem Phys* 10:11017–11096. doi:[10.5194/acp-10-11017-2010](https://doi.org/10.5194/acp-10-11017-2010)
- Lohmann U, Feichter J (2005) Global indirect aerosol effects: a review. *Atmos Chem Phys* 5:715–737
- Mani A, Chacko O, Hariharan S (1969) A study of Ångström turbidity parameters from solar radiation measurements in India. *Tellus* 21:829–843
- McComiskey A, Schwartz SE, Schmid B, Guan H, Lewis ER, Ricchiazzi P, Ogren JA (2008) Direct aerosol forcing: calculation from observables and sensitivities to inputs. *J Geophys Res* 113:D09202. doi:[10.1029/2007JD009170](https://doi.org/10.1029/2007JD009170)
- Meehl GA, Arblaster JM, Collins WD (2008) Effects of black carbon aerosols on the Indian Monsoon. *J Climate* 21:2869–2882
- Menon S, Hansen J, Nazarenko L, Luo Y (2002) Climate effects of black carbon aerosols in China and India. *Science* 297:2250–2253
- Moorthy KK, Satheesh SK, Krishna Murthy BV (1997) Investigations of marine aerosols over the tropical Indian Ocean. *J Geophys Res* 102:18827–18842
- Moorthy KK, Babu SS, Badarinath KVS, Sunilkumar SV, Kiranchand TR, Ahmed YN (2007) Latitudinal distribution of aerosol black carbon and its mass fraction to composite aerosols over peninsular India during winter season. *Geophys Res Lett* 34:L08802. doi:[10.1029/2006GL029150](https://doi.org/10.1029/2006GL029150)
- Moorthy KK, Nair VS, Babu SS, Satheesh SK (2009) Spatial and vertical heterogeneities of aerosol radiative forcing over the oceanic regions surrounding the Indian peninsula: climate implications. *Q J R Meteorol Soc* 135:2131–2145
- Moorthy KK, Beegum SN, Srivastava N, Satheesh SK, Chin M, Blond N, Babu SS, Singh S (2013) Performance evaluation of chemistry transport models over India. *Atmos Environ* 71:210–225
- Nair VS, Satheesh SK, Moorthy KK, Babu SS, George SK, Nair PR (2010) Surprising observation of large anthropogenic aerosol fraction over the near-pristine southern Bay of Bengal: climate implications. *J Geophys Res Atmos* 115:D21201. doi:[10.1029/2010JD013954](https://doi.org/10.1029/2010JD013954)
- Nair VS, Solmon F, Giorgi F, Mariotti L, Babu SS, Moorthy KK (2012) Simulation of South Asian aerosols for regional climate studies. *J Geophys Res Atmos*. doi:[10.1029/2011JD016711](https://doi.org/10.1029/2011JD016711)
- Nair VS, Babu SS, Moorthy KK, Sharma AK, Marinoni A, Ajai (2013a) Black carbon aerosols over the Himalayas: direct and surface albedo forcing. *Tellus B* 65:19738
- Nair VS, Babu SS, Moorthy KK, Prijith SS (2013b) Spatial gradients in aerosol-induced atmospheric heating and surface dimming over the oceanic regions around India: anthropogenic or natural? *J Clim* 26:7611–7621
- Nair VS, Babu SS, Moorthy KK, Satheesh SK (2014) Implications of multiple scattering on the assessment of black carbon aerosol radiative forcing. *J Quant Spectrosc Radiat Transf* 148:134–140
- Nigam S, Bollasina M (2010) The ‘elevated heat pump’ hypothesis for the aerosol-monsoon hydroclimate link: “grounded” in observations? *J Geophys Res* 115:D16201
- Novakov T, Kirchstetter TW, Menon S, Aguiar J (2008) Response of California temperature to regional anthropogenic aerosol changes. *Geophys Res Lett* 35:L19808. doi:[10.1029/2008GL034894](https://doi.org/10.1029/2008GL034894)
- Pant P, Hegde P, Dumka UC, Sagar R, Satheesh SK, Moorthy KK (2006) Aerosol characteristics at a high altitude location in central Himalayas: optical properties and radiative forcing. *J Geophys Res* 111:D17206. doi:[10.1029/2005JD006768](https://doi.org/10.1029/2005JD006768)
- Pathak B, Kalita G, Bhuyan K, Bhuyan PK, Moorthy KK (2010) Aerosol temporal characteristics and its impact on shortwave radiative forcing at a location in the northeast of India. *J Geophys Res* 115:D19204. doi:[10.1029/2009JD013462](https://doi.org/10.1029/2009JD013462)
- Peng J et al (2016) Markedly enhanced direct radiative forcing of black carbon particles under polluted urban environments. *Proc Natl Acad Sci USA* 113(16):4266–4271
- Porter JN, Miller M, Pietras C, Motell C (2001) Ship-based sun photometer measurements using Microtops sun photometers. *J Atmos Ocean Technol* 18:765–774
- Ramachandran S, Kedia S (2010) Black carbon aerosols over an urban region: radiative forcing and climate impact. *J Geophys Res* 115:D10202. doi:[10.1029/2009JD013560](https://doi.org/10.1029/2009JD013560)
- Ramanathan V, Crutzen PJ, Lelieveld J, Mitra AP, Althausen D, Anderson J, Andreae MO, Cantrell W, Cass GR, Chung CE, Clarke AD, Coakley JA, Collins WD, Conant WC, Dulac F, Heintzenberg J, Heymsfield AJ, Holben B, Howell S, Hudson J, Jayaraman A, Kiehl JT, Krishnamurti TN, Lubin D, McFarquhar G, Novakov T, Ogren JA, Podgorny IA, Prather K, Priestley K, Prospero JM, Quinn PK, Rajeev K, Rasch P, Rupert S, Sadourny R, Satheesh SK, Shaw GE, Sheridan PJ, Valero FPJ (2001) Indian Ocean experiment: an integrated analysis of the climate forcing and effects of the great Indo-Asian haze. *J Geophys Res* 106:28371–28398
- Ramanathan V, Chung C, Kim D, Bettge T, Buja L, Kiehl JT, Washington WM, Fu Q, Sikka DR, Wild M (2005) Atmospheric brown clouds: impacts on South Asian climate and hydrological cycle. *Proc Natl Acad Sci* 102:5326–5333
- Ricchiazzi P, Yang S, Gautier C, Sowle D (1998) SBDART: a research and teaching software tool for plane-parallel radiative transfer in the Earth’s atmosphere. *Bull Am Meteorol Soc* 79:2101–2114
- Satheesh SK, Srinivasan J (2006) A method to estimate aerosol radiative forcing from spectral optical depths. *J Atmos Sci* 63:1082–1092
- Satheesh SK, Moorthy KK, Kaufman YJ, Takemura T (2006) Aerosol optical depth, physical properties and radiative forcing over the Arabian Sea. *Meteorol Atmos Phys* 91:45–62. doi:[10.1007/s00703-004-0097-4](https://doi.org/10.1007/s00703-004-0097-4)
- Satheesh SK, Moorthy KK, Babu SS, Vinoj V, Dutt CBS (2008) Climate implications of large warming by elevated aerosols over India. *Geophys Res Lett* 35:L19809. doi:[10.1029/2008GL034944](https://doi.org/10.1029/2008GL034944)
- Satheesh SK, Torres O, Remer LA, Babu SS, Vinoj V, Eck TF, Kleidman RG, Holben BN (2009) Improved assessment of aerosol absorption using OMI-MODIS joint retrieval. *J Geophys Res*. doi:[10.1029/2008JD011024](https://doi.org/10.1029/2008JD011024)
- Schulz M, Textor C, Kinne S, Balkanski Y, Bauer S, Bernsten T, Berglen T, Boucher O, Dentener F, Guibert S, Isaksen ISA, Iversen

- T, Koch D, Kirkevåg A, Liu X, Montanaro V, Myhre G, Penner JE, Pitari G, Reddy S, Seland Stier P, Takemura T (2006) Radiative forcing by aerosols as derived from the AeroCom present-day and pre-industrial simulations. *Atmos Chem Phys* 6:5225–5246
- Soni VK, Attri SD, Taneja K, Peshin SK (2014) Assessment of aerosol radiative properties in India. *Met Monograph IMD*, No: ESSO/IMD/EMRC/01/2014
- Vinoj V, Rasch PJ, Wang H, Yoon J, Ma PL, Landu K, Singh B (2014) Short-term modulation of Indian summer monsoon rainfall by West Asian dust. *Nat Geosci* 7:308–313. doi:[10.1038/ngeo2107](https://doi.org/10.1038/ngeo2107)
- Wang S-H, Lin N-H, Chou M-D, Woo J-H (2007) Estimate of radiative forcing of Asian biomass-burning aerosols during the period of TRACE-P. *J Geophys Res* 112:D10222. doi:[10.1029/2006JD007564](https://doi.org/10.1029/2006JD007564)
- Wang Y, Khalizov A, Levy M, Zhang R (2013) New directions: light absorbing aerosols and their atmospheric impacts. *Atmos Environ* 81:713–715
- Wang Y, Lee K-H, Lin Y, Levy M, Zhang R (2014) Distinct effects of anthropogenic aerosols on tropical cyclones. *Nat Clim Change* 4:368–373
- Wang Y, Jiang J, Su H (2015) Atmospheric responses to the redistribution of anthropogenic aerosols. *J Geophys Res Atmos* 120(18):9625–9641
- Yu H, Dickinson RE, Chin M, Kaufman YJ, Zhou M, Zhou L, Tian Y, Dubovik O, Holben BN (2004) Direct radiative effect of aerosols as determined from a combination of MODIS retrievals and GOCART simulations. *J Geophys Res* 109:D03206. doi:[10.1029/2003JD003914](https://doi.org/10.1029/2003JD003914)
- Zhang R, Wang G, Guo S, Zamora M, Lin Y, Wang W, Hu M, Wang Y (2015) Formation of urban fine particulate matter. *Chem Rev* 115(10):3803–3855